Acoustics Today

Vertical Line Array
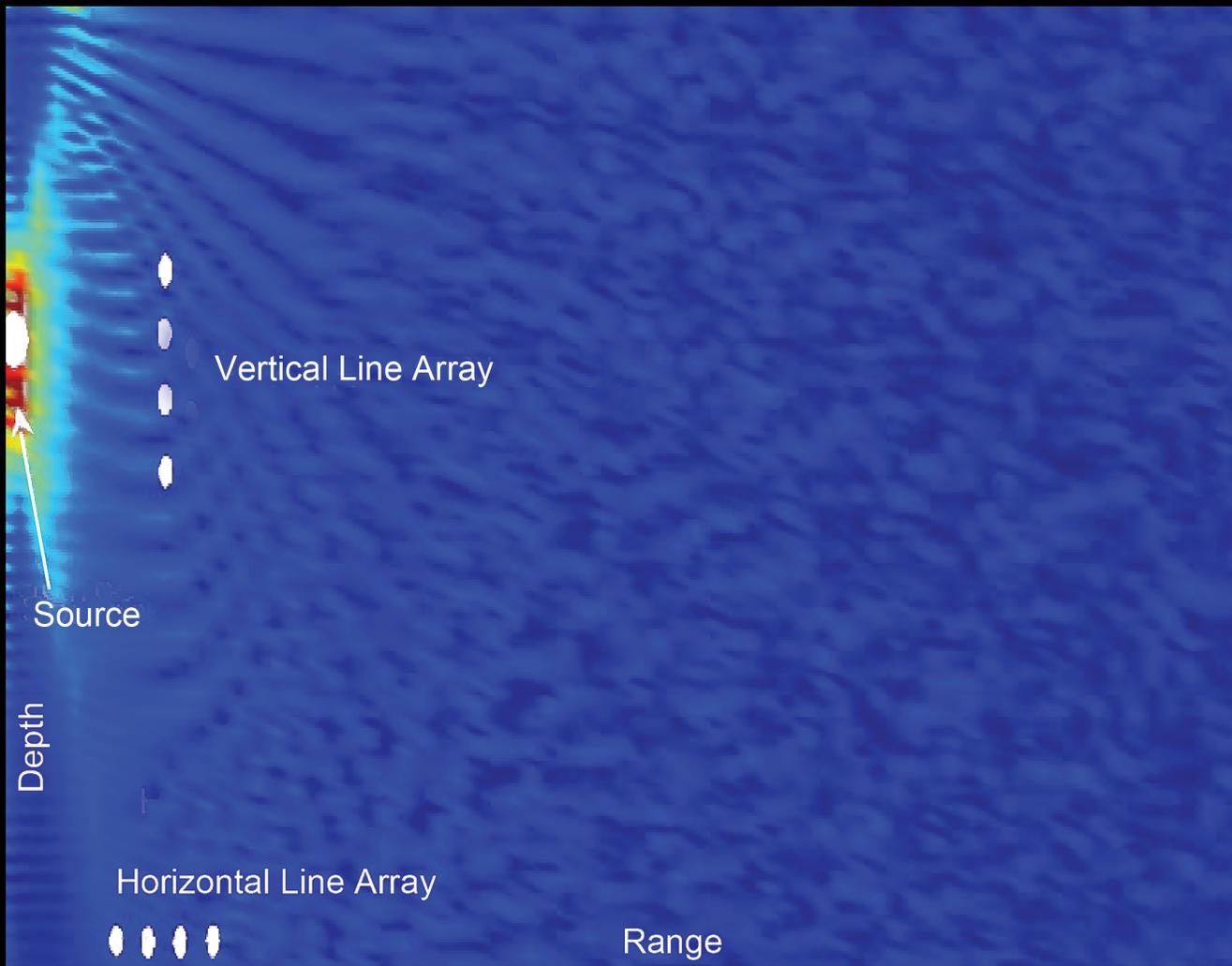
Source

Depth

Horizontal Line Array

Range

Model-Based Ocean Acoustics
Physical and Engineering Acoustics
Speech and Hearing Technology
Animal Bioacoustics
and more

A publication of
the Acoustical Society
of America

Signal Processing in Acoustics

SIGNAL PROCESSING IN PHYSICAL AND ENGINEERING ACOUSTICS

David H. Chambers
Lawrence Livermore National Laboratory
Livermore, California, 94551

Brian E. Anderson
Acoustics Research Group, Department of Physics and Astronomy
Brigham Young University
Provo, Utah 84602

Brian G. Ferguson, Kam W. Lo
Maritime Operations Division—Sydney, Defense Science and Technology Organization
Pyrmont, 2009 New South Wales, Australia

Michael J. Roan
Department of Mechanical Engineering
Virginia Polytechnic Institute and State University
Blacksburg, Virginia 24061

Introduction

Signal processing is used extensively in physical and engineering acoustics, with applications in nondestructive evaluation, machine and structural monitoring, tracking and localization, and elsewhere. The goal of signal processing is to extract desired information from noisy and uncertain measurements. In this process we exploit both statistical analysis and properties of acoustic wave generation and propagation to separate extraneous components of the measurements from the signal of interest. To illustrate signal processing in physical and engineering acoustics, we present three examples of signal processing that illustrate different methods and approaches to the problem of extracting desired information from measurements. The first example uses the symmetry of reciprocal wave propagation and timing of reflections to detect flaws (cracks) in plates. This is an illustration of a signal processing technique that exploits a principle associated with physical acoustics. The second example uses a sophisticated statistical approach to determine the condition of gears in a gearbox from accelerometer measurements. Machine condition monitoring is a large area of engineering acoustics—motivated by both cost and safety. The final example shows how combining information from different sound sources improves the ability to locate the origin of a bullet fired from a firearm.

"Signal processing is used extensively in physical and engineering acoustics, with applications in nondestructive evaluation, machine and structural monitoring, tracking and localization, and elsewhere."

Time reversal

Time reversal (TR)[1] is a method of locating and characterizing sources and to intentionally focus energy at a selected location in space.[2,3] The original time reversal experiments were conducted by Parvulescu and Clay in the early 1960s to demonstrate the reproducibility of signal transmissions in the ocean.[4] The technique has found applications in SONAR,[5] communications,[6,7] medical ultrasound,[8,9] nondestructive evaluation,[10,11] and seismic imaging[12,13] (see selected references for recent work in these areas). The application of TR to nondestructive evaluation allows localization of cracks,[10] which are nonlinear scatterers, and linear passive scatterers.[11] It will likely soon be shown that TR can be used to locate acoustic emission events, as work-in-progress continues.

To illustrate the application of TR to nondestructive evaluation, we will describe a basic TR experiment. During the forward propagation step, a source signal is broadcast from location *A* in a bounded sample. A reversible transducer at location *B* collects the directly propagated signal from *A* and reflections of the source signal from the various possible reflected paths between *A* and *B*. The signal recorded at *B* is then reversed in time and during the backward propagation step is broadcast from the reversible transducer at *B*. This second broadcast signal traverses the propagation paths traversed during the forward propagation step. The energy broadcast along each respective path is timed such that they will simultaneously arrive at *A*.

Reverse time migration (RTM) is a variant of TR commonly used in seismology applications to image scatterers of interest in the ground. Anderson *et al.* recently demonstrated that RTM may be fully implemented experimentally in 2-D laboratory samples to image scatterers on an inaccessible side of a laminated plate in places where these scatterers may partially be due to delamination.[11] To image scatterers using RTM, the aforementioned TR experiment is carried out as normal, however during both the forward and backward propagation steps the vibration of the wave field at various points within a region of interest (ROI) must be sensed, (with a scanning laser vibrometer for example). RTM imaging correlates the arrivals of energy at specific times at a particular scatterer during the forward propagation with corresponding arrivals of energy at analogous times at the same scatterer during the broadcast and convergence of energy of the back-
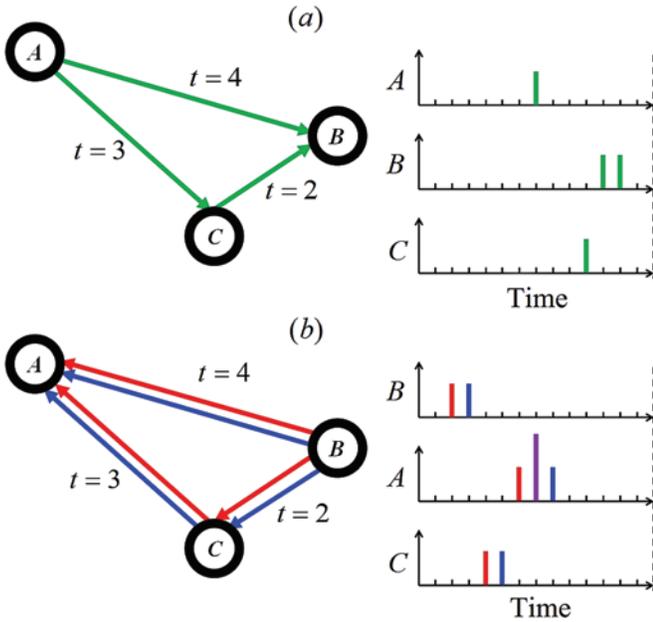
Fig. 1. Illustration of the reverse time migration process in a free space with a scatterer at location C. The propagation times for each path are included for the reader's reference. (a) Forward propagation step. (b) Backward propagation step.

ward propagation (after these last set of data have been reversed in time). To the degree that the energy broadcast during the backward propagation step retraces the forward propagation paths, RTM allows imaging of passive scatterers.

Figure 1a illustrates the forward propagation of a RTM experiment conducted in free space with a source at A, a reversible transducer at B and a scatterer at C. The forward signal is emitted from A after 7 time units. This forward signal is then directly received at B at a time of 11 units and the reflection off of C arrives at B at a time of 12 units. The forward signal arrives at C at a time of 10 units. The signal recorded at B is now flipped in time and used as the source signal for the backward propagation depicted in Fig. 1b (we color the two emission signals from B to aid visualization of this step). The red signal from B directly travels to A and arrives at a time of 6 units. The red signal from B also reflects off C and arrives at A at a time of 7 units. The blue signal from B also directly travels to A and arrives at a time of 7 units (constructively interfering with the reflected red arrival producing the purple recorded signal). The blue signal from B also reflects off of C and arrives at A at a time of 8 units. The signal at A is typical of a symmetric time reversal focus signal.[14] The signal recorded at C consists of the red signal delayed by 2 time units and the blue signal delayed by 2 units. Now, if the signal recorded at C is reversed in time and compared to the signal recorded at C during the forward propagation step, one will notice that the green arrival and the red arrival are synced in time. The traditional RTM image, I, is found through computing the cross correlation of the forward signal, F, at position (x,y) with the backward signal, B, at (x,y), after this later signal has been reversed in time,

$$I_{x,y} = \mathfrak{I}^{-1}\left[\mathfrak{I}\{F_{x,y}(t)\}\mathfrak{I}^*\{B_{x,y}(-t)\}\right],\qquad(1)$$

where $\mathfrak{I}$ represents a Fourier transform, * represents phase

conjugation, and $-t$ represents a time reversal. The magnitude of the image $|I_{x,y}|$ is then typically displayed to locate scatterers. Anderson *et al.* found that this traditional imaging condition does not work well in a highly reverberant medium and instead used the following imaging condition with better results

$$M_{x,y} = \mathfrak{I}^{-1}\left[\left|\mathfrak{I}\{F_{x,y}(t)\}\mathfrak{I}^*\{B_{x,y}(-t)\}\right|\right].\qquad(2)$$

The experiments conducted by Anderson *et al.* found that scatterers of a high impedance relative to the sample impedance showed up as minima in the $M_{x,y}$ image. In another experiment at the Los Alamos National Laboratory, the question of whether $M_{x,y}$ could distinguish between low and high density scatterers was investigated[15]. This experiment utilized a nearly semicircular aluminum plate of dimensions 6.54x179x396 mm (pictured in Fig. 2a). The characters "LANL" are milled out of the plate at a depth of 3.23 mm and a width of 10 mm. The characters "EES-11" are cut out of a 2.64 mm thick steel plate with a width of 10 mm and glued onto the plate. The removal of plate material for the "LANL" characters should present an incident wave with a low impedance scatterer, while the addition of material for the "EES-11" characters should present a high impedance scatterer. In this experiment a single transducer (labeled as S in Fig. 2a and is slightly not in view for the photograph) is used as the source with a single receiver transducer (labeled as R
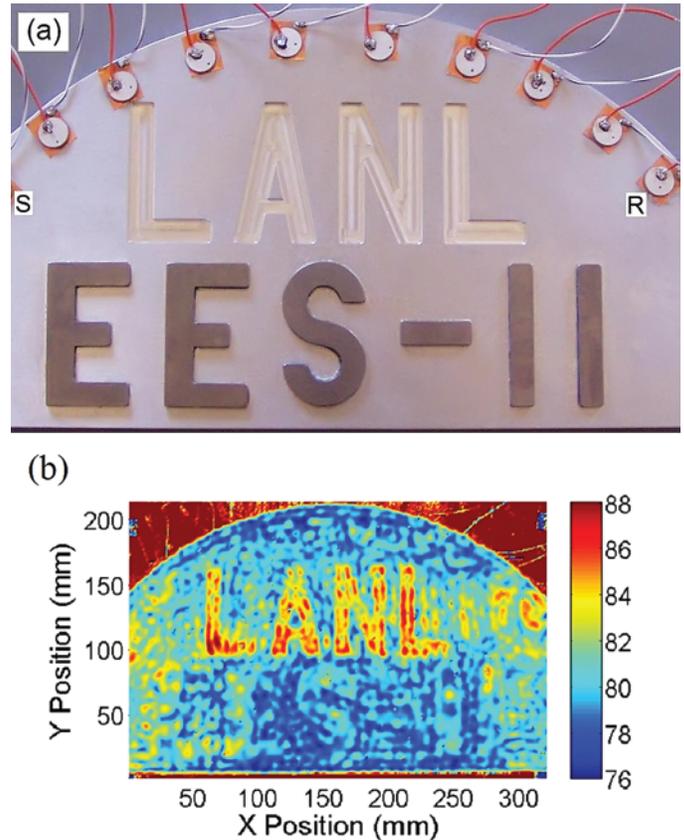

Fig. 2. (a) Photograph of a semicircular aluminum plate which has the letters "LANL" milled out of it and steel letters "EES-11" glued onto it[15]. S and R denote the source and receiver transducers named according to the forward propagation usage. (b) RTM image of the other side of this plate (mirror image is displayed). Amplitude is in dB units with an arbitrary reference.

in Fig. 2a). A scanning laser vibrometer scans the forward and backward propagation wave fields on the other side of the plate. The ROI in this experiment includes all of the characters with approximately a 1 mm spacing between scan points. The image $M_{x,y}$ of the characters is displayed in Fig. 2b. The characters "LANL" are clearly visible as maxima of $M_{x,y}$. The characters "EES-11" are not quite as visible. It is expected that these would show up as minima just as the high impedance scatterers used in the work of Anderson *et al*. The reason for the poorly visible "EES-11" characters may be due to the thickness of the plate relative to the wavelength, resulting in a smaller impedance contrast from the "EES-11" letters to the aluminum plate than the impedance contrast in the Anderson *et al*. experiments.

Thus, RTM imaging for nondestructive evaluation of bounded plate samples may be used to image passive scatterers and locations of disbonding of those scatterers. This procedure may be carried out to image scatterers on the opposite side of a thin plate if that side is inaccessible. It may also prove to distinguish between high and low impedance scatterers. The work of Anderson *et al*. illustrated that high impedance scatterers showed up as minima in an RTM image and the work presented here shows that low impedance scatterers show up as maxima, but further work needs to be done to determine why the high impedance scatterers considered here did not show up as minima.

Independent component analysis applied to non-invasive gear health monitoring

The non-invasive monitoring of the health of gearboxes[16] has been a very active area of research over the past two decades. The capability to predict gear failures from accelerometer-based measurements of the gear meshing vibration signal is of great importance in industries such as the aerospace industry (e.g., helicopter gearboxes). If one can predict failure, then gears can be swapped during regular scheduled maintenance. This prevents accidents and saves money due to unscheduled down time. The main concept in gear health monitoring is that the meshing of the gear and pinion (Fig. 3) gives rise to a vibration signal that propagates to the gearbox case where it is measured by accelerometers. The challenge is that, in real systems, many vibration signals arise due to vehicle motion, shaft imbalances, mode shape vibrations of the gearbox case, etc. All of these are also present at the measurement points necessitating the development of signal processing approaches that can isolate and analyze the gear mesh signal from the undesired signals (noise). Past condition-monitoring techniques of gearboxes have used many different signal processing approaches such as synchronous time series averaging,[17] amplitude and phase demodulation,[18] time–frequency distribution,[19] and wavelet analysis.[20] The use of statistical signal processing approaches have also taken hold in gear tooth failure detection.[21] Non-linear adaptive algorithms for independent component analysis (ICA) have been shown to separate unknown, statistically independent sources that have been mixed in dynamic systems. This example illustrates the application of an information maximization based blind-
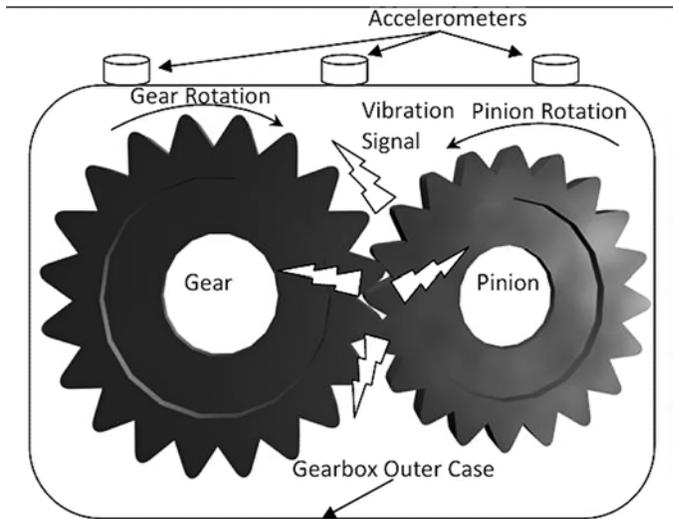

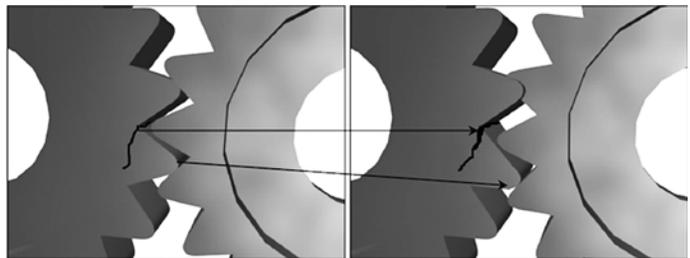Fig. 3. Simple spur gear and pinion setup.

Fig. 4. Crack formation and growth at the base of a gear tooth.

source separation algorithm (a type of independent component analysis) to the prediction of gear failures. It is shown that ICA can be used to detect impulsive and random changes in the gear vibration data.

In typical gearbox setups, the pinion drives the gear through rotational motion where force is exerted on the gear teeth where the pinion teeth come into contact with the gear teeth. A common failure of the gear teeth occurs when a crack occurs at the base of the tooth due to material fatigue (Figure 4).

The crack formation at the base of the tooth begins to cause the tooth to flex when the pinion exerts force on the tooth. Because the tooth flexes, there is a slight delay in the rotation of the gear causing a modulation of the meshing vibration signal. It is this modulation that fault monitoring algorithms attempt to detect before the tooth actually fails.

Having measured the signals at several locations on the gearbox surface, the next task is to separate the gear-pinion meshing signal and determine whether a change (or modulation) occurs during the gear-pinion contact period. One candidate algorithm for performing these tasks is the blind-source separation algorithm (BSS).

Figure 5 shows a high level diagram of the BSS algorithm. The approach assumes that there are r independent source signals that are linearly mixed by a mixing matrix A. This linear mixing is the mathematical model for signals from multiple sources arriving at each accelerometer. The signals X(t) are then measured at the accelerometer points and fed into the BSS part of the algorithm. BSS attempts to minimize the mutual information between accelerometer channels (i.e., measurements made at several points on the
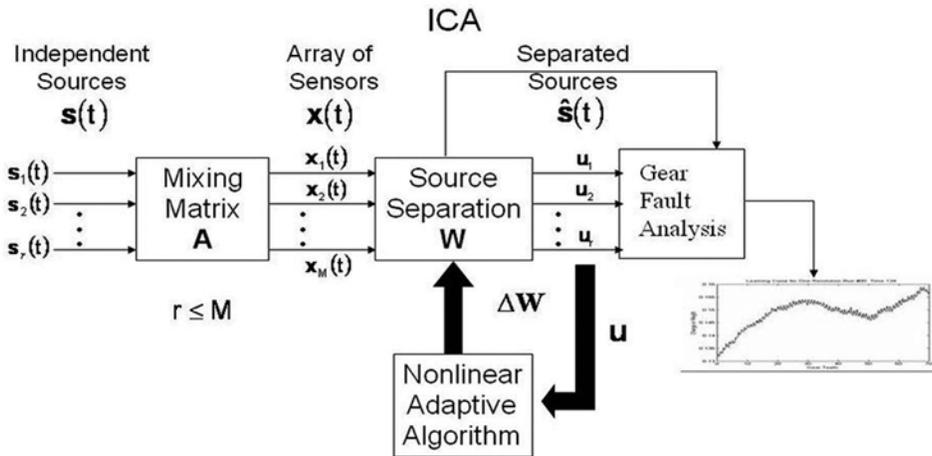
Fig. 5. High level diagram of the Blind Source Separation Algorithm.

gearbox surface). This forces the independent sources Ŝ into separate channels. The weight matrix W, once learned, is ideally A⁻¹. By observing changes in the trace of the weight matrix W, one can observe points where the algorithm diverges (i.e., where there are abrupt statistical changes in the signals). By plotting the trace of W as a function of the gear tooth locations, the modulation of the meshing signal can be detected. Figure 6 gives a plot of the trace of W versus gear tooth number for a healthy gear and for the same gear at a later time as it begins to fail. The point of the future failure is very visible in the lower plot. This approach provides the possibility to non-invasively monitor the health of gears or other types of rotating machin-

ery such as bearings using measurements made at the gearbox (or machine) surface and can in theory separate out all of the unwanted signals that are present in the mixture of signals at the measurement points. This allows an analysis of the "clean" signatures alone. This is the reason that ICA/BSS algorithms have seen wide application from voice processing to the isolation of sounds in the human chest cavity.

Acoustical signal processing methods for localizing gunshots

To an unalerted listener, the sound of gunfire represents an aural event in the soundscape that evokes a reaction of surprise tempered by curiosity. However, in engineering acoustics it represents a transient acoustic signal generated by the discharge of a firearm from which information can be extracted such as the location of the point of fire[22] (*localization*) and the type of firearm (*classification*). The sound pulse generated by the discharge of a bullet from a firearm is referred to as the *muzzle blast* or in military parlance—the *report*. The acoustic energy propagates at the speed of sound travel in air and expands as a spherical wavefront (of constant phase) centered on the point of fire. Because the propagation of the sound through the atmosphere is omnidirectional, it can be heard from any direction, even behind the firer. If the listener is positioned forward (towards the front) of the firer *and* the bullet travels at supersonic speed, then a second transient signal, which is referred to as the *(ballistic) shock wave* is heard. To the listener, the origin of the shock wave occurs at a point *Pn* (referred to as the *detach point*), which is located at a distance x_n along the trajectory of the bullet—see Fig. 7. When the listener is near the trajectory, the sound pulse (or sonic boom) is extremely loud. Similar to the muzzle blast wave, the shock wavefront
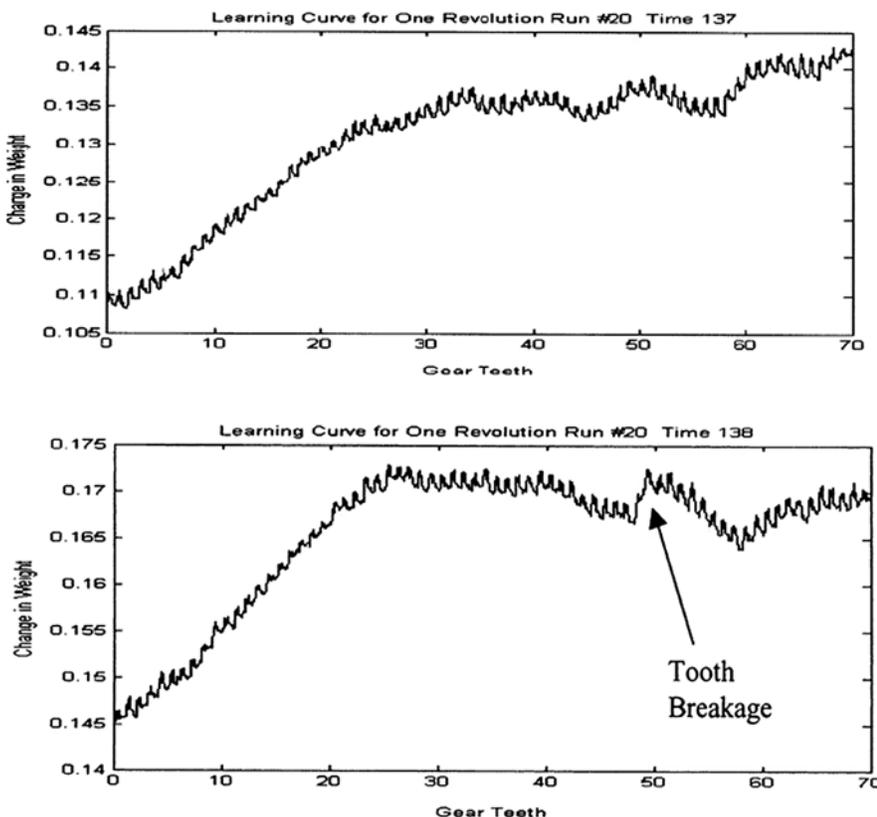

Fig. 6. Result of Blind Source Separation Processing for a healthy gear (top) and for a gear that is beginning to break (bottom).
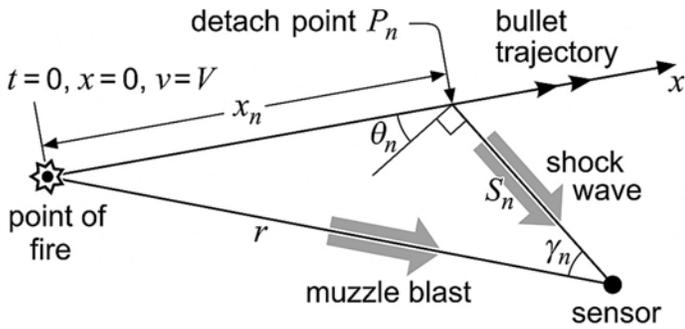
Fig. 7. Acoustic transient signals–the muzzle blast is generated at the point of fire and the ballistic shock wave originates from the detach point along the bullet's trajectory.

travels away from its point of emission at the speed of sound. But, unlike the muzzle blast wavefront, it expands as a conical surface with the trajectory and nose of the bullet defining the axis and apex of the cone respectively. The angle θ_n (see Fig. 7) at the apex of the cone is referred to as the *Mach angle*, whose sine is equal to the reciprocal of the Mach number, which is defined as the ratio of the bullet's speed v to the speed of sound c.[23] A casual listener will hear the shock wave *before* the muzzle blast and instinctively look in the direction of its origin (the detach point) and confuse it with the actual direction of the firer, which coincides with the direction of the muzzle blast that arrives later—see Fig 7.

By sensing these signals at spatially-separated sensors and applying various acoustical signal processing methods for sound source localization, it is possible to estimate the position of the firing point. One method, which relies *only* on the muzzle blast, is referred to as *passive ranging by wavefront curvature*.[24] The simplest sensor configuration for this method consists of three equally-spaced microphones positioned along a straight line—see Fig. 8. The basic principle is
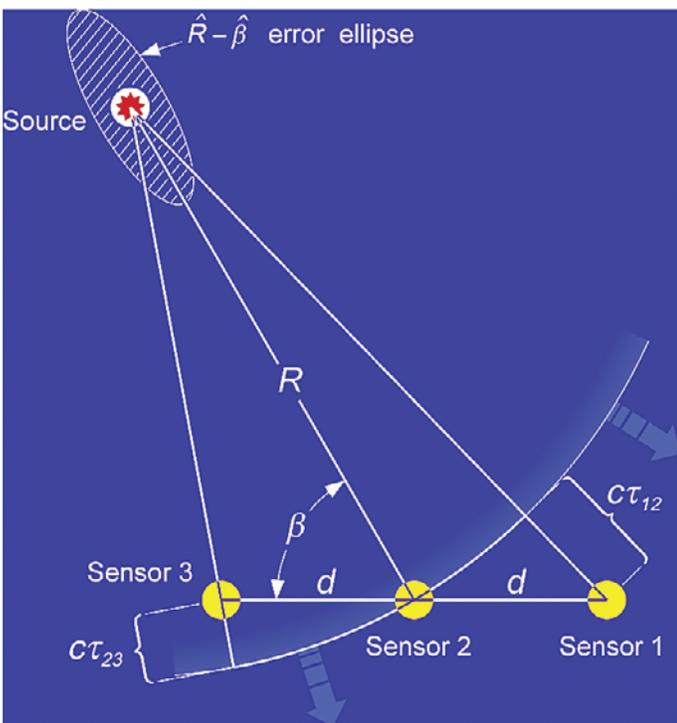

Fig. 8. Source-sensor geometry for passive ranging by wavefront curvature.

to estimate the wavefront's radius of curvature, which corresponds to the range of the firing point. Knowing the speed of sound travel in the atmosphere (c) and the intersensor separation distance (d), and measuring the differences in the arrival times (τ_{12} and τ_{23}) of the muzzle blast wavefront at adjacent sensor pairs, enables the calculation of the source range R (from the middle sensor) and source bearing β (with respect to the array axis).[24] The results of applying this method to the passive ranging of real gunshot data from five different firing positions are shown in Fig. 9; typically 260 rounds were fired from each position. The variance of the source range estimates increases with range, while the bearing estimates for the serial conducted at the longest range (475 m) have a bias error which could be attributed to atmospheric refraction of the sound or uncertainty in the ground truth data of the firing position. The variances of both the range and bearing estimates can be reduced by increasing the *effective* sensor separation distance ($d \sin \beta$).[24]

A second method, which uses *both* muzzle blast and shock wave information, is referred to as the *ballistic model-based method* for passive ranging of direct fire weapons.[25] Measuring the differences in the arrival times ($\Delta\tau_n = r/c - t(x_n)$-
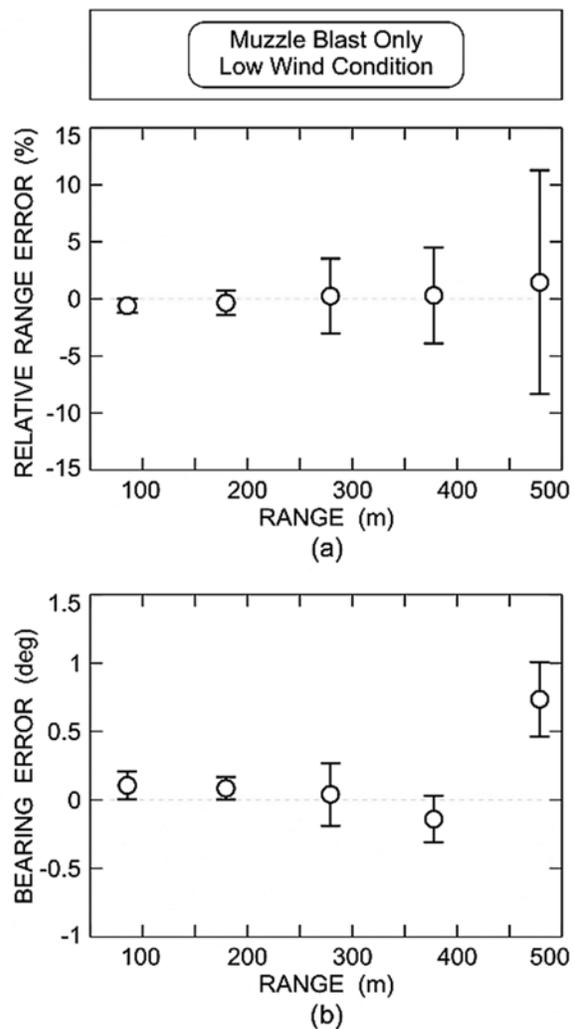

Fig. 9. Variation with range of (a) relative range error and (b) bearing error for localizing the point of fire at five ranges using passive ranging by wavefront curvature of the muzzle blast wave only.
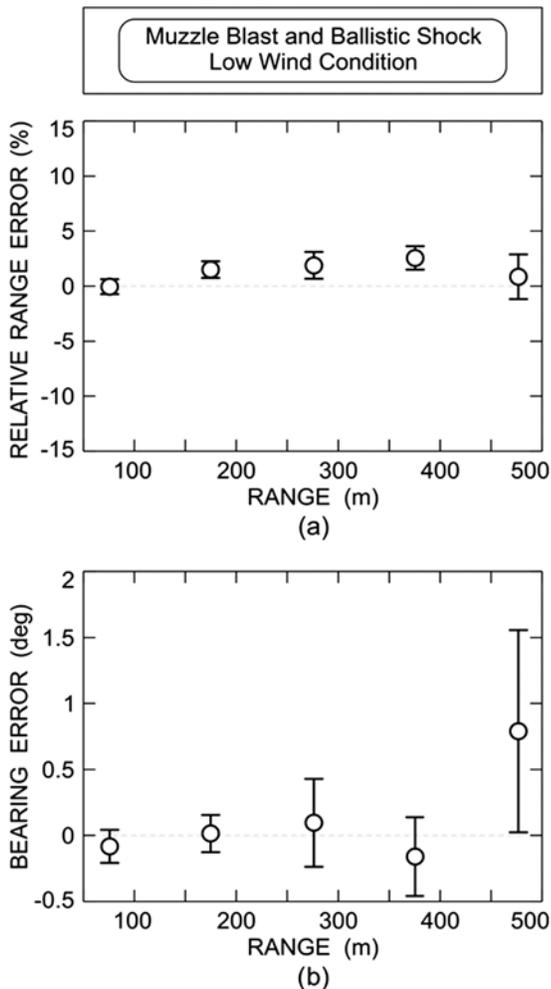
Fig. 10. Similar to Fig. 9 but for the ballistic model-based method which uses both the muzzle blast and shock wave information.

s_n/c) and arrival angles γ_n of the muzzle blast and shock waves at a sensor node n (a small baseline sensor array) enables the range r to be estimated—see Fig. 7. For a bullet travelling with a constant velocity (V), the range is,[25] $r=c\Delta\tau_n/(1-\cos\gamma_n)$. In practice, range estimates based on the constant bullet velocity assumption can have significant errors (especially at long source ranges), necessitating the development of a ballistic model-based approach that accounts for the deceleration of the bullet along its trajectory. The shock wavefront is better represented (visualized) as a half prolate spheroid (pointed oval shape like an American football) for a decelerating bullet, rather than as a conical surface for a bullet travelling with a constant velocity. The ballistic parameters, which must be known *a priori* or estimated *in situ*, are the bullet's initial velocity and the ballistic constant (which depends on the bullet's mass, cross-sectional area and aerodynamic drag). The results of applying this method to the passive ranging of real gunshot data from the five different firing positions are shown in Fig. 10. When compared with the passive ranging by wavefront curvature method (Fig. 9), the variances of the ranges of the firing positions are reduced when estimated using the ballistic model-based method, most notably at the longer source ranges. The converse is true for the bearings of the source positions

because of the shorter baseline of the sensor array used with the ballistic model-based method. Additionally, when the source ranges are estimated using the conventional method which assumes a constant bullet velocity, they are found to have significant bias errors especially at the longer firing ranges. Also, the radial error, which is defined as the separation distance between the estimated and actual firing positions, is found to be dependent on the caliber of the bullet—the conventional method's radial errors are much larger for 5.56 mm rounds than for 7.62 mm caliber ammunition.

Currently under development is a third localization method[26] that relies *only* on the ballistic shock wave information, which is advantageous when the received muzzle blast is absent due to the use of a sound suppressor (*silencer*) or weak due to the high transmission loss (spreading loss plus absorption loss) suffered by the acoustic signal when its propagation path from source to sensor is long. Another advantage of this method occurs when there is simultaneous fire from different firing positions as each shock wave signal is not required to be associated with a corresponding muzzle blast signal as is the case with the ballistic model-based method. A new method proposed by the authors is *simultaneous localization and classification*, which uses both the muzzle blast and shock wave information received by a next-generation network of spatially-distributed unattended ground sensors comprising "*low-cost sensor nodes operating on shoestring power budgets for years at a time in potentially hostile environments without hope of human intervention.*"

Summary

In this article we have presented three examples of signal processing approaches in physical and engineering acoustics. In time reversal, we exploit a principle in physical acoustics to enhance the detection of flaws in plates and structures. In gearbox monitoring we show how sophisticated statistical techniques such as principle component analysis and blind source separation can be employed to solve a difficult and important problem in structural and machine monitoring. Finally, in point of fire localization we see how both wavefront curvature and shock front propagation can be combined to improve estimates of the origin of a bullet fired from a gun. We hope this gives a flavor of the variety of approaches and applications of signal processing to physical and engineering acoustics.**AT**

Acknowledgments

References

1   For more information contact author B.E.A. Electronic mail: bea@byu.edu
2   M. Fink, "Time reversed acoustics," Physics Today **50**, 34–40 (1997).
3   B. E. Anderson, M. Griffa, C. Larmat, T. J. Ulrich, and P. A. Johnson, "Time reversal," Acoustics Today **4**(1), 5–16 (2008).
4   A. Parvulescu and C. S. Clay, "Reproducibility of signal trans-

mission in the ocean," Radio and Electrical Engineering **29**, 223–228 (1965).

5 K. G. Sabra, P. Roux, H.-C. Song, W. S. Hodgkiss, W. A. Kuperman, T. Akal, and J. M. Stevenson, "Experimental demonstration of iterative time-reversed reverberation focusing in a rough waveguide. Application to target detection," J. Acoust. Soc. Am. **120**(3), 1305–1314 (2006).

6 H.-C. Song, J. S. Kim, W. S. Hodgkiss, W. A. Kuperman, and M. Stevenson, "High-rate multiuser communications in shallow water," J. Acoust. Soc. Am. **128**(5), 2920–2925 (2010).

7 H.-C. Song, W. S. Hodgkiss, and P. A. van Walree, "Phase-coherent communications without explicit phase tracking," J. Acoust. Soc. Am. **128**(3), 969–972 (2010).

8 J. L. Robert and M. Fink, "Green's function estimation in speckle using the decomposition of the time reversal operator: Application to aberration correction in medical imaging," J. Acoust. Soc. Am. **123**(2), 866–877 (2008).

9 S. Dos Santos and Z. Prevorovsky, "Imaging of human tooth using ultrasound based chirp-coded nonlinear time reversal acoustics," Ultrasonics **51**(6), 667–674 (2011).

10 B. E. Anderson, M. Griffa, T. J. Ulrich, P.-Y. Le Bas, R. A. Guyer, and P. A. Johnson, "Crack localization and characterization in solid media using time reversal techniques," American Rock Mechanics Association, #10–154 (2010).

11 B. E. Anderson, M. Griffa, P.-Y. Le Bas, T. J. Ulrich, and P. A. Johnson, "Experimental implementation of reverse time migration for nondestructive evaluation applications," J. Acoust. Soc. Am. Express Lett. **129**(1), EL8–EL14 (2011).

12 C. Larmat, R. A. Guyer, and P. A. Johnson, "Tremor source location using time reversal: Selecting the appropriate imaging field," Geophysical Research Lett. **36**, L22304 (2009).

13 C. Larmat, R. A. Guyer, and P. A. Johnson, "Time reversal methods in seismology," Physics Today **63**(8), 31–35 (2010).

14 T. J. Ulrich, M. Griffa, and B. E. Anderson, "Symmetry-based imaging condition in time reversed acoustics," J. Applied Physics **104**(6), 064912 (2008).

15 B. E. Anderson, M. Griffa, L. Huang, P. A. Johnson, P.-Y. Le Bas, and T. J. Ulrich, "A comparison of time reversal imaging techniques of two dimensional samples," XIII International Conference on Nonlinear Elasticity and Materials, Aix en Provence, France, June (2008).

16 For more information contact author M.J.R. Electronic mail: mroan@vt.edu.

17 M. Lebold, K. McClintic, R. Campbell, C. Byington, and K. Maynard, "Review of vibration analysis methods for gearbox diagnostics and prognostics," in *Proceedings of the 54th Meeting of the Society for Machinery Failure Prevention Technology*, Virginia Beach, VA, 623–634 (2000).

18 J. E. Nicks and G. Krishnappa, "Gear fault detection using modulation analysis techniques," IMechE Conference Transactions: 2nd International Conference on Gearbox Noise, Vibration and Diagnostics, May1995, 81–89.

19 W. J. Wang and P. D. McFadden, "Early detection of gear failure by vibration analysis," Mech. Sys. and Signal Process. **7**, 193–203 (1993).

20 A. J. Miller, "A new wavelet basis for the decomposition of gear motion error signals and its application to gearbox diagnostics," M.S. thesis, The Graduate School of The Pennsylvania State University (1999).

21 M. J. Roan, J. Erling, and L.H. Sibul, "A new, non-linear, blind source separation algorithm for gear tooth failure analysis," J. Mech. Systems and Signal Process. **16**(5), 719–740 (2002).

22 For more information contact authors B.G.F. and K.W.L. Electronic mail: Brian.Ferguson@dsto.defence.gov.au, Kam.Lo@dsto.defence.gov.au

23 A. D. Pierce, *Acoustics – An Introduction to Its Physical Principles and Applications* (Acoustical Society of America, Melville, NY, 1994) pp. 606–615.

24 B. G. Ferguson, "Variability in the passive ranging of acoustic sources in air using a wavefront curvature technique," J. Acoust. Soc. Am. **108**(4), 1535–1544 (2000).

25 K. W. Lo and B. G. Ferguson, "A ballistic model-based method for ranging direct fire weapons using the acoustic muzzle blast and shock wave," *Proceedings of the 2008 Intelligent Sensors, Sensor Networks and Information Processing Conference*, CD ISBN: 978-1-4244-2957-8. pp. 453–458.

26 K. W. Lo and B. G. Ferguson, "Acoustic methods for localizing small arms fire," J. Acoust. Soc. Am. (submitted September 2011).

David H. Chambers received a Bachelor's of Science in physics in 1980, and subsequently a Master's in physics and a Bachelor's in mechanical engineering in 1982, all from Washington University in St. Louis. He received a Ph.D. in Theoretical and Applied Mechanics with an emphasis in Applied Mathematics in 1988 from the University of Illinois Urbana-Champaign. Since then he has been a physicist and electrical engineer at Lawrence Livermore National Laboratory. Over his career, he has published articles in many technical areas including laser propagation through turbulence, evaluation of techniques for extracting coherent structure information from turbulent fluid flows, signal processing of dispersive waves, and acoustic time reversal. He is presently working on radar imaging and detection, nondestructive evaluation, and signal processing models of radiation transport. He is a Fellow of the Acoustical Society of America. In his spare time he enjoys hiking and exploring the beach with his family (pictured).

Brian Anderson is visiting assistant professor of acoustics in the Physics and Astronomy Department of Brigham Young University (BYU). Prior to his appointment at BYU, he was a postdoctoral research associate in the Geophysics Group (EES-17) at the Los Alamos National Laboratory. He earned his Ph.D. in Acoustics from The Pennsylvania State University in 2006. He earned M.S. and B.S. degrees in Physics from BYU where he began his study of the field of acoustics. Brian is actively involved in the Acoustical Society of America (ASA) running the Gallery of Acoustics competition, redesigning the website for the Technical Committee on Signal Processing in Acoustics, and chairing sessions and giving talks at ASA meetings. As a student he served on the ASA Student Council. Besides his passion for all things acoustics he enjoys geocaching, wood working, and many sports. Most of all he enjoys spending time with his wife Angela and their three boys Travis, Lucas, and Marcus. His sons have learned at early ages to generate and listen to impulse responses (by clapping) whenever they are in reverberant spaces.

Brian G. Ferguson is Principal Scientist and Engineer responsible for Acoustic Systems Science in the Maritime Operations Division of Australia's Defense Science and Technology Organisation. He is Australia's national leader in Battlespace Acoustics under the Technical Cooperation Program between the Governments of Australia, Canada, New Zealand, the United Kingdom, and the United States. He is also an invited member of the North Atlantic Treaty Organization (NATO) Sensors and Electronics Technology Panel TG-53. His work has been published widely in international scientific and engineering journals. He was the General Chair of the OCEANS '10 Institute of Electrical and Electronics Engineers (IEEE) Conference and Exhibition held at the Sydney Convention and Exhibition Centre, Darling Harbour, 24-27 May 2010. Dr Ferguson is a Fellow of the Acoustical Society of America, a Senior Member of the Australian Institution for Radio and Electronics Engineers, a Chartered Professional Engineer, a Member of the Australian Institution of Engineers and a Senior Member of the Institute of Electrical and Electronics Engineers. He was a recipient of the NATO Research and Technology Organization 2009 Scientific Achievement Award.

Kam W. Lo is a Senior Research Scientist in the Maritime Operations Division of Australia's Defense Science and Technology Organization, where he is responsible for the development of advanced signal processing algorithms in support of acoustic systems science having defense applications. His work has been published widely in international journals and conference proceedings. He was the Technical Program Chair of OCEANS '10 IEEE, Sydney. Dr. Lo is a Senior Member of the Institute of Electrical and Electronics Engineers.

Michael Roan received B.S., M.S., and Ph.D. degrees from The Pennsylvania State University. He is currently the John Jones III Professor of Mechanical Engineering at Virginia Poly-technic Institute and State University. Previous to his appointment at Virginia Tech, he was the head of the Signal Processing Department at the Applied Research Laboratory at Penn State. His current areas of research include statistical signal processing for distributed detection and estimation systems, blind source separation, adaptive signal processing methods, and information fusion for heterogeneous data streams.